Journal of The Electrochemical Society, **152** (6) H74-H79 (2005)
0013-4651/2005/152(6)/H74/6/$7.00 © The Electrochemical Society, Inc.

Electrically Biased NO_x Sensing Elements with Coplanar Electrodes

David L. West,*,z Fred C. Montgomery, and Timothy R. Armstrong*

Oak Ridge National Laboratory, Oak Ridge, Tennessee 37831, USA

Fabrication and characterization of electrically biased NO_x sensing elements operative at 500–600°C are described. The sensing elements were produced by screen-printing Pt and transition metal oxide electrodes on yttria-stabilized zirconia substrates. DC electrical biasing greatly enhanced the response of the sensing elements to nitric oxide (NO), with voltage changes on the order of 10% observed as the sensing response to 450 ppmv NO at 600°C and 7 vol % O_2. Voltage and current biasing techniques were employed with a sensing element using $NiCr_2O_4$ as the oxide, and the computed changes in resistance due to NO were nearly identical, suggesting that the response mechanism of the elements is a change in dc electrical resistance. The sensing response was minimally affected by O_2 concentrations between 7 and 20 vol % at [NO] concentration levels from 0 to 1500 ppmv. These sensing elements and techniques may be useful in sensors for measuring [NO] at temperatures near 600°C.
 [DOI: 10.1149/1.1901003]

Manuscript submitted May 26, 2004; revised manuscript received August 30, 2004. Available electronically April 22, 2005. This was Paper 914 presented at the San Antonio, Texas, Meeting of the Society, May 9-14, 2004.

Environmental stewardship is driving efforts to control emissions from mobile power sources such as automobile and truck engines. The primary pollutants of concern (setting aside the greenhouse gas CO_2) are hydrocarbons, CO, NO_x, and SO_x. SO_x can be ameliorated by using low-sulfur fuel and hydrocarbons and CO can be remediated by oxidation on a catalyst. NO_x, however, has so far proved resistant to decomposition in excess oxygen, which is a barrier to emissions control of the O_2-rich exhausts from diesel and lean-burn gasoline engines.

If a lean NO_x catalyst is not developed, technologies such as NO_x traps or selective catalytic reduction (SCR) will be required for NO_x remediation. Both of these approaches will require on-board NO_x sensors, either to control regeneration of the NO_x trap or reagent injection in SCR. A suitable sensor would be operative at temperatures around 600–700°C, able to measure NO_x in the range 10 ppmv $\leqslant [NO_x] \leqslant$ 1000 ppmv, and would be relatively insensitive to varying $[O_2]$.[1,2] It is important to recognize that the two dominant NO_x species above room temperature are the mono- and dioxide, NO and NO_2. NO_2 is favored thermodynamically at room temperature, but NO is the dominant equilibrium species above about 500°C.[3]

Currently, two different compact and robust NO_x sensors for mobile power applications have been described in the literature: an amperometric[2,4,5] sensor produced by NGK[6] and a mixed-potential[7,8] sensor produced by Riken.[9] Both sensors are based on yttria-stabilized zirconia (YSZ) and consist of several cavities. In the NGK design, the O_2 in the exhaust gas is removed in the first cavity (thus driving the NO/NO_2 equilibrium toward NO), and the NO removed electrochemically in a subsequent cavity. The current measured during the electrochemical removal is linearly related to the $[NO_x]$ of the exhaust. The Riken design is also multicavity and one of the cavities contains an NO_2 conversion electrode, which converts the NO_x in the exhaust to NO_2 before impingement on the mixed-potential sensing electrode. The conversion is required because NO_2 and NO typically induce voltages of opposite signs with mixed-potential sensing elements.[10] In both cases the voltage is proportional to $\ln[NO_x]$.

In this work we are investigating the use of dc electrical biasing in NO_x sensing elements. This was studied by Miura *et al.*[11] who applied fixed dc voltages (in the range 0.1-0.5 V) to both tubular and plate-shaped YSZ sensing elements consisting of one Pt electrode and one $CdCr_2O_4$-coated Pt electrode. In the tubular design only the $CdCr_2O_4$-coated electrode was exposed to the NO_x-containing gas while in the plate design both electrodes were exposed to the NO_x. The dc current (I) between the electrodes was shown to be a measure of the $[NO_x]$ for both designs, and selectivity for NO was demonstrated for the tubular design at 500°C. No data was reported at other temperatures.

Ho *et al.*[12] applied dc voltages to a sensing element consisting of Nd_2CuO_4 and Pt electrodes on opposite sides of a YSZ disk. As was the case in the work of Miura *et al.* at 500°C, the presence of NO_x produced an increase in I at 400°C. dc voltage biasing of elements similar to those described by Ho *et al.* was also explored by Grilli *et al.*,[13] except $LaFeO_3$ was used as the oxide electrode. Again, the presence of NO_2 increased the magnitude of I (at 450°C). Finally, Coillard *et al.*[14] applied a dc voltage to a $MgAl_2O_4$-coated sensing element consisting of interdigitated Pt electrodes on YSZ. In atmospheres with low $[O_2]$ (800-1800 ppm), NO produced an increase in I between the electrodes at 700°C, but larger amounts of oxygen (>1 vol %) led to no change being observed in I due to the presence of NO.

The present investigation explores the use of both voltage and current biasing techniques with YSZ-based sensing elements. In particular, we were concerned with the effect of biasing sign and magnitude on the NO and NO_2 responses, the use of both fixed-voltage and current biasing, and the effect(s) of the oxygen contents typically encountered in diesel engine exhausts ($\sim$5-20%[15,16]). Several different oxides were employed in sensing elements of nominally identical geometry in order to search for commonalities that might guide rational sensing element design. The investigation was confined to temperatures $\geqslant$500°C, as this is at the low end of the desired operating temperatures for the mobile power applications cited previously, and we focused on sensing elements with coplanar electrodes.

Experimental

Figure 1a shows schematically the sensing element geometry selected for the present investigation. The design was influenced in part by the work of Miura *et al.*[11] The YSZ (TZ-8Y, Tosoh) substrate was produced by tape casting, laminating, and sintering at 1400°C for 2 h in air. These procedures yielded a sintered ceramic with $\rho/\rho_{th} \geqslant 98\%$. A Pt (Electroscience) layer, which comprised fully one electrode and the bottom layer of the other, was then screen-printed on one side of the YSZ disk, air-dried, and fired at 1100°C for 20 min in air. Finally, an oxide layer was screen-printed over a portion of one of the Pt electrodes, air-dried, and fired at 900°C for 15 min in air. Several different oxides were employed in the prototype sensing elements and these are listed in Table I, along with the identifications that are used throughout this document. The oxides in

* Electrochemical Society Active Member.
z E-mail: westdl@ornl.gov

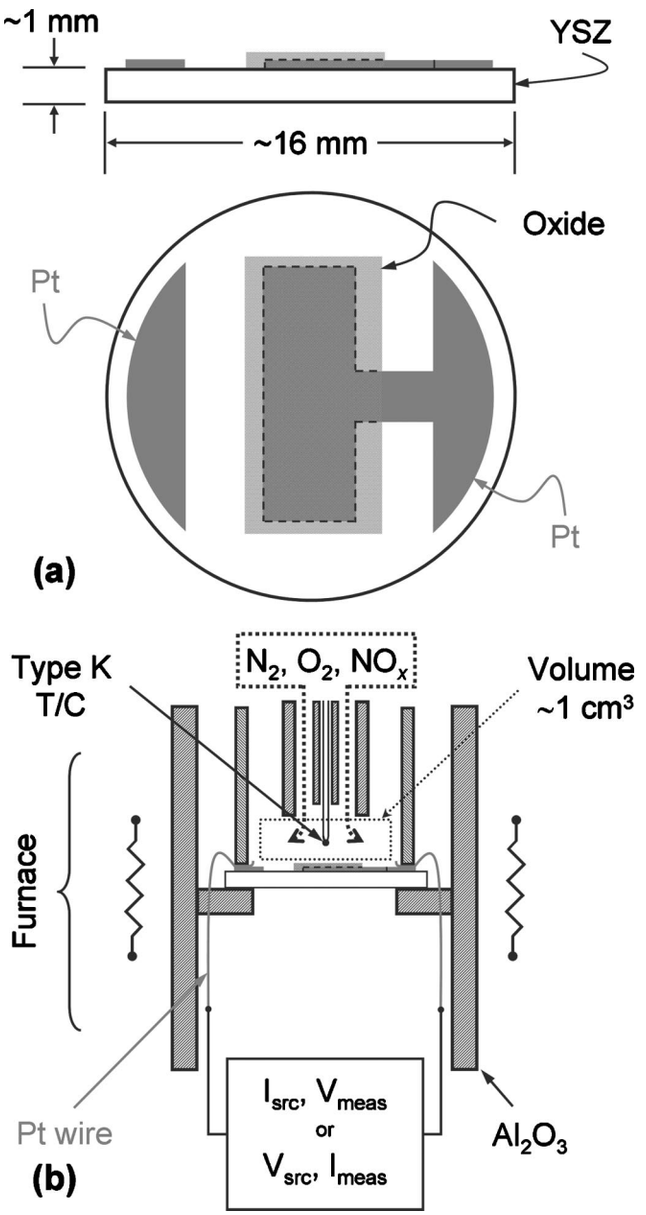

Figure 1. Schematic of (a) sample geometry and (b) test fixture. The type-K thermocouple shown in (b) was used strictly for monitoring, not temperature control of the furnace.

Table I were all obtained commercially, except the $NiFe_2O_4$ which was synthesized in-house by combustion synthesis.[17]

NO_x sensing performance of the prototype elements was evaluated using the apparatus shown schematically in Fig. 1b. The sensing element was placed, centrally located, in a resistively heated furnace. (The furnace temperature was controlled by a type K thermocouple placed next to the heating elements, not the thermocouple shown in Fig. 1b.) A commercial four-inlet gas mixer (Environics 4000, not shown) was used to mix N_2, O_2, and either NO or NO_2 (5000 ppm in N_2) at room temperature. These gas mixtures were then presented to the electroded side of the sensing element, and a chemiluminescent NO_x meter (TEI 42C, also not shown) was used to measure the NO_x concentrations (at room temperature) in the gas mixtures after exiting the furnace. A dc bias, either current or voltage, was maintained across the element electrodes using either a Keithley 2400 (current bias) or 6517 (voltage bias). In the case of current biasing, the dc voltage between the electrodes was monitored while in the case of voltage biasing the dc current between the electrodes was monitored.

Table I. Oxides employed as electrode materials and sensing element identifications.

Oxide	Source	Element ID
$NiCr_2O_4$	Cerac	$NiCr_2O_4$
$NiFe_2O_4$	Synthesized in house	$NiFe_2O_4$
$Ba_{0.08}Cu_{1.92}Cr_2O_5$	Aldrich	BCCr
$CuWO_4$	Cerac	$CuWO_4$
$La_{0.8}Ca_{0.2}CrO_3$	Praxair	LCC

Five types of experiments were carried out, with the first being preliminary in nature. This first experiment consisted of measuring the exit NO_x concentrations as the total flow through the apparatus was varied from 0.25 to 1.75 L/min at a furnace temperature of 600°C. This was done in order to characterize how the NO_x concentrations in the test gas might be changing upon mixing at room temperature, flowing through the elevated temperature furnace, and then subsequently cooling back to room temperature upon exiting the furnace. No bias was applied to the sensing element during this test.

The second and third types of tests were designed to study the effect of biasing sign and magnitude on the NO_x responses. Bias sweeps were conducted (in which the current applied to the sensing element was stepped at discrete levels (*e.g.*, −0.2,−0.1,0.0,+0.1, +0.2 mA) under atmospheres of 0 ppmv NO_x and 450 ppmv NO or NO_2 (7 vol % O_2 in all cases). The voltage readings were then compared at each bias level to deduce a measure of the voltage change caused by NO and NO_2. In the second type of bias sweep, the current was again stepped but the timing was synchronized with the gas mixing unit, and 450 ppmv pulses of NO or NO_2 (2 min in duration) were applied during the 5 min spent at each bias level. These two types of tests consistently revealed the same general conclusion for the effect of bias sign and magnitude on the NO_x responses.

The final investigations described herein were conducted at fixed bias levels. First, $[NO_x]$ and $[O_2]$ were systematically varied at a constant dc bias, temperature, and flow rate. Finally, the effect of flow rate on the sensing response was investigated by varying the flow rate at constant T, $[O_2]$, and input [NO] as described previously, but with a fixed current bias applied to the sensing element.

Results and Discussion

Effect of flow rate on exit NO_x concentrations.—Figure 2 shows how the measured NO_x concentrations (at the exit of the furnace) varied with flow. Strongly flow-dependent decomposition of NO_2 (to NO) was observed, whereas for the case of input NO, the NO_x measured in the exit stream was typically ~90% NO if the flow was greater than 0.5 L/min. The interpretation adopted was that decomposition of NO_2 to NO in the furnace (T = 600°C) was a more serious difficulty than formation of NO_2 from NO and O_2 in the room temperature lines leading to and from the furnace. Given the data in Fig. 2 and the desired NO_x concentrations in the test gas (~10 to ~1000 ppm) relative to the capabilities of the available mass flow controllers, 0.75 L/min was selected as the flow rate for the following three portions of the investigation.

Effect of current bias on the NO_x response.—The typical effect of current-biasing sign and magnitude on the NO_x responses of the sensing elements is shown in Fig. 3 for data collected at 500°C from a sensing element made with Ba-modified $Cu_2Cr_2O_5$ (BCCr) as the oxide. When the multilayered electrode in Fig. 1a was biased negatively with respect to the bare Pt electrode (−25 μA), the introduction of 450 ppmv NO_2 or NO (in 7 vol % O_2) caused a decrease in

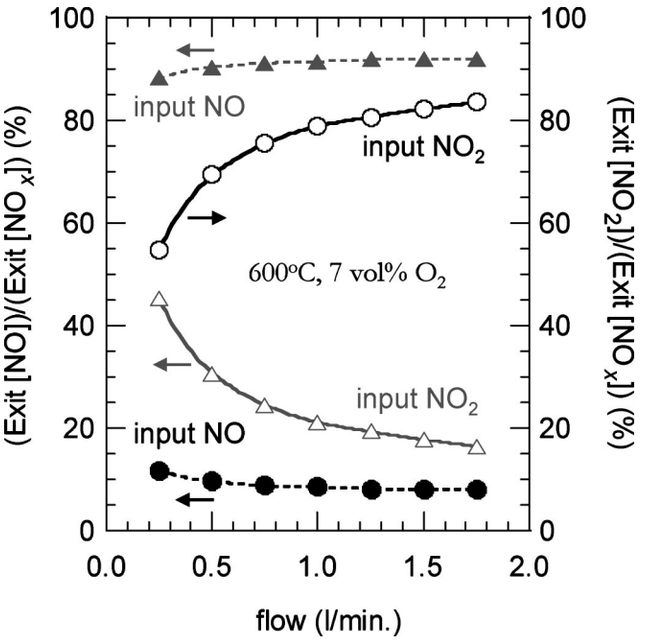

Figure 2. Dependence of measured exit $[NO_x]$ on flow rate. The data shown were collected at a furnace temperature of 600°C with either 450 ppmv NO or NO_2 as the input NO_x in 7 vol % O_2.

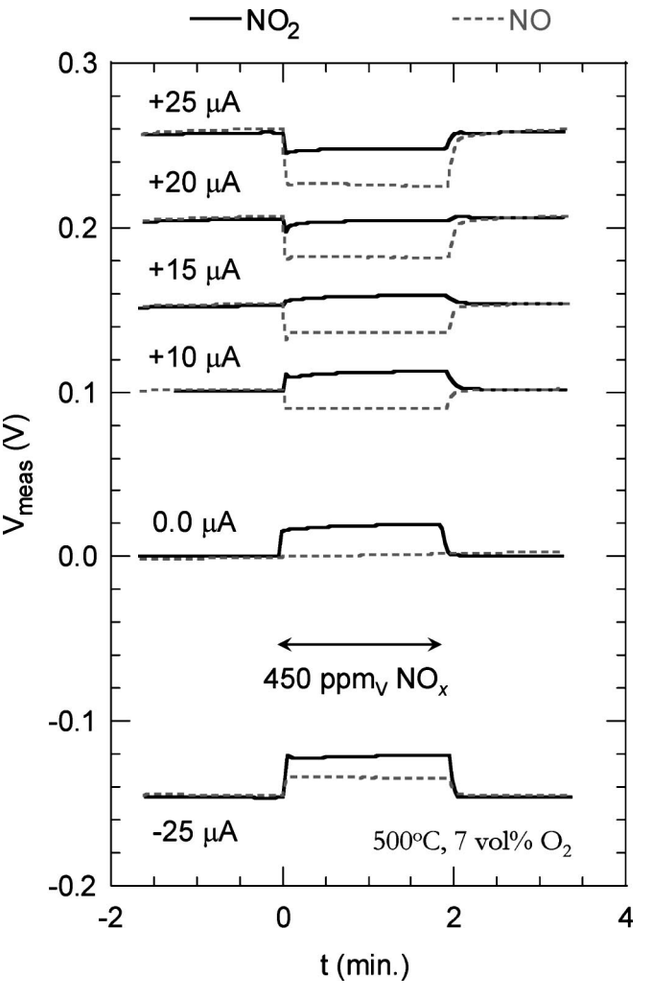

Figure 3. Measured NO and NO_2 response traces (500°C, 7 vol % O_2) at different current biases. Data collected from the BCCr sensing element of Table I.

the magnitude of the measured dc voltage, indicating a decrease in resistance. At small positive biases ("+10, +15 μA"), the introduction of 450 ppmv NO causes a decrease in the measured voltage, but the introduction of the same concentration of NO_2 causes an increase. As the bias is increased, the introduction of NO_2 causes smaller increases in the measured voltage and eventually leads to a decrease, but of a smaller magnitude than that caused by NO (the data labeled 25 μA in Fig. 3). Because the NO_2 response is first an increase in V at small positive biases and then a decrease at larger biases, there must be a bias at which the response is zero. For the BCCr sensing element in Fig. 3, this bias is about +20 μA.

Figure 4 shows that the general behavior illustrated by the BCCr sensing element in Fig. 3 was exhibited by all the sensing elements listed in Table I. Consistently the changes in voltage (ΔV) induced by 450 ppmv NO_2 were large and positive at negative biases, and increasing positive bias drives $\Delta V_{450\ \text{ppmv}\ NO_2}$ to zero and eventually negative. When NO is the input NO_x species, 450 ppmv NO causes a decrease in $|V_{meas}|$ (smaller than that observed for 450 ppmv NO_2) at negative biases, and a decrease in V_{meas} at positive biases.

It is noteworthy that some of the voltage changes in Fig. 4 are quite large on a percentage basis relative to the NO_x concentrations apparently causing them. For example, the $NiCr_2O_4$ sensing element, at 600°C and +0.1 mA bias, showed a 26 mV voltage change when exposed to 450 ppmv NO (Fig. 4c). This a 13% change relative to the background voltage measured in the absence of NO_x (~200 mV, Fig. 4d). Therefore a component present in the atmosphere at a volume percentage of 0.045 is causing an approximate 300-fold larger (in terms of percentage) change in the measured voltage.

An attempt can be made to analyze the behavior observed in Figs. 3 and 4 by considering the possible electrochemical reactions involving NO_x, O_2, and the current carrying species in the Pt (electrons) and the YSZ electrolyte (oxygen ions). The possible NO_x and O_2 reduction reactions with these species are

$$NO + 2e^- \rightarrow \tfrac{1}{2}N_2 + O^{2-} \quad [1]$$

$$NO_2 + 2e^- \rightarrow NO + O^{2-} \quad [2]$$

and

$$\tfrac{1}{2}O_2 + 2e^- \rightarrow O^{2-} \quad [3]$$

while the possible oxidation reactions are

$$NO + O^{2-} \rightarrow NO_2 + 2e^- \quad [4]$$

and

$$O^{2-} \rightarrow \tfrac{1}{2}O_2 + 2e^- \quad [5]$$

where all molecular species are gaseous and O^{2-} represents an oxygen ion in the YSZ solid electrolyte.

The directions of motion for the various current-carrying species (electrons and oxygen ions) are shown schematically under conditions of positive and negative bias in Fig. 5. With negative biases, both NO_2 and NO cause a drop in the magnitude of V, indicating a decrease in resistance, as less voltage is required to maintain the current. This would seem to indicate facile oxidation of NO (Eq. 4) on the bare Pt electrode (as oxidation must occur on this electrode for current to flow) and reduction of NO_2 (Eq. 2) on the partially oxide-covered Pt electrode.

With positive biases, the analysis is less straightforward. The decrease in voltage typically observed with NO can again be attributed to oxidation of NO (Eq. 4), this time on the oxide-covered Pt

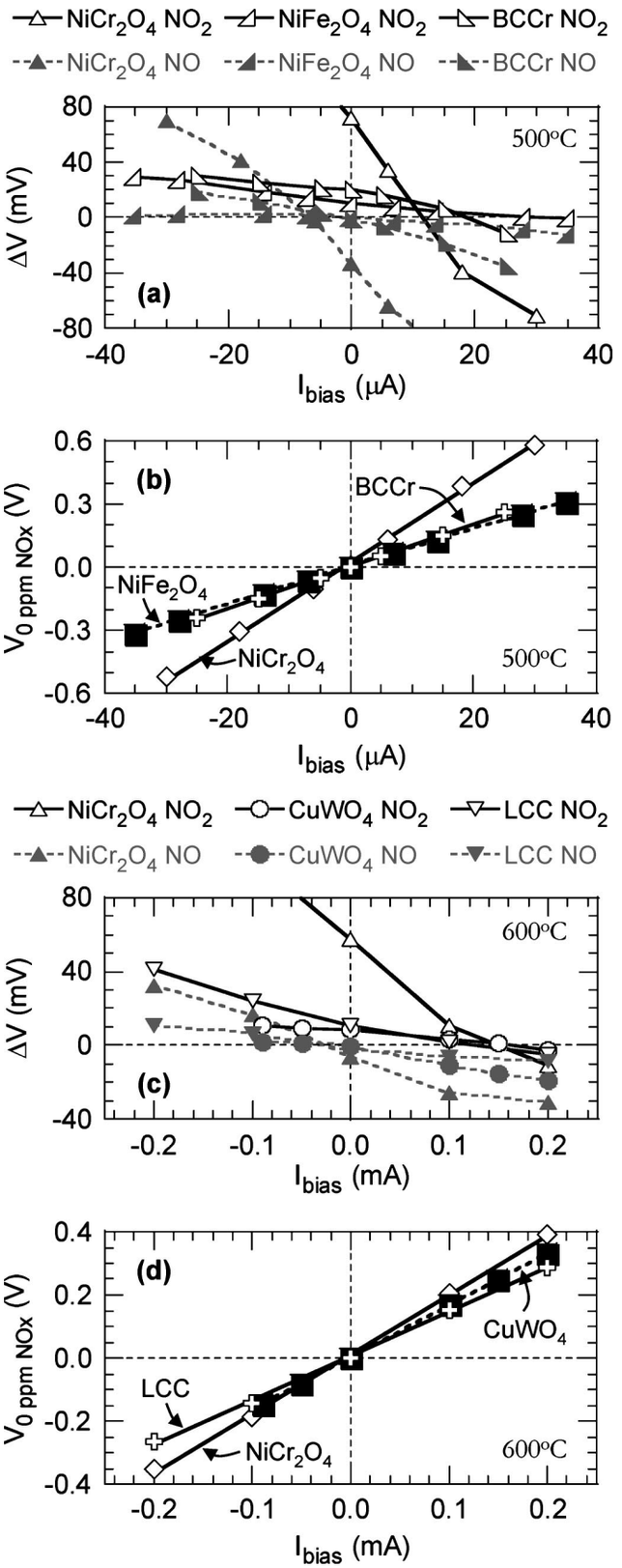

Figure 4. Changes in measured voltage (ΔV) induced by 450 ppmv NO_x (7 vol % O_2, balance N_2) at (a) 500 and (c) 600°C. Lines in (a) and (c) are drawn as an aid to the eye. (b and d) Show measured *V-I* curves in 7 vol % O_2, balance N_2 at 500 and 600°C, respectively. The lines drawn in (b) and (d) are linear fits.

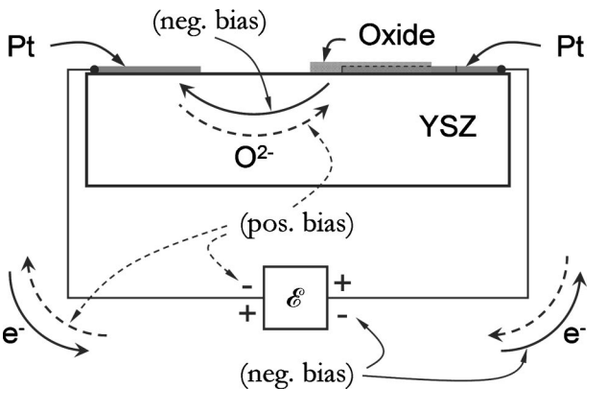

Figure 5. Schematic of current [electron (e^-) and oxygen ion (O^{2-})] flow with positive and negative biases. $\mathcal{E}$ represents a dc power supply.

electrode. The increase in voltage (corresponding to an increase in resistance) observed at smaller positive biases with NO_2 defies such a simple explanation. In the absence of NO_2, for current to flow oxygen must be oxidized (to O_2 gas, Eq. 5) at the partially oxide-covered electrode and reduced (Eq. 3) at the bare Pt electrode. It is possible that NO_2 absorbs competitively with O_2 at the Pt electrode and cannot undergo reduction. Another possibility, suggested by Miura *et al.*,[11] is that NO_2 can still be reduced at the "anode" (the oxide-covered electrode) at small positive biases, and this interferes with the oxidation of oxygen ions. Perhaps the explanation offered by Miura *et al.* is more plausible, because as shown in Fig. 3 and 4 for sufficiently large positive biases, NO_2 no longer causes an increase in the measured voltage, rather a small decrease.

The data in Fig. 4 show that for the $NiCr_2O_4$ sample the voltage changes induced by 450 ppmv NO_x are smaller at 600 than 500°C (particularly on a percentage basis). In general, it was always found for the sensing elements in Table I that increasing temperature led to smaller responses, and the $NiFe_2O_4$ and BCCr elements in Fig. 4a and b showed virtually no NO response at 600°C. Although this decreasing response with temperature is unfortunate from the standpoint of the desired application, it does lend credence to the explanation offered for the NO response, as the ability to oxidize NO to NO_2 should be increasingly difficult as the temperature increases above 500°C.

Figure 6a and b shows the response of the LCC sensing element (biased with +0.2 mA) as the input NO and then NO_2 were varied at constant $[O_2]$ (7 vol %). The asymmetry in the NO and NO_2 response that was observed at 450 ppmv in Fig. 4c holds over the concentration range 300 ppmv $\leqslant [NO_x] \leqslant$ 1500 ppmv. Similar behavior for the $CuWO_4$ sensing element is shown over an even wider concentration range in Fig. 6c. Data such as that shown in Fig. 6 suggest that it may be possible to design NO-selective sensing elements, but we consider that just the strong NO response of these sensing elements is noteworthy. As mentioned earlier, a NO_x sensor that is near commercialization[9] employs a NO_2 conversion electrode to take advantage of the much stronger NO_2 response of mixed-potential sensing elements.[2] Because NO is the dominant equilibrium NO_x species at temperatures above 500°C, sensor design could be simplified if sensing elements with a strong response to NO were employed. Therefore, here we report further only on characterization performed with NO as the input NO_x and focus on the oxide in Table I that gave the strongest NO response: $NiCr_2O_4$.

Current vs. voltage biasing.—All the data reported above were obtained with current-biased sensing elements. In order to ascertain whether the method of biasing (current or voltage) affected sensing element response, a $NiCr_2O_4$ sensing element was biased at +0.10 mA and subjected to systematic variations in [NO] at two fixed O_2 concentrations (7 and 13 vol %). The same element was

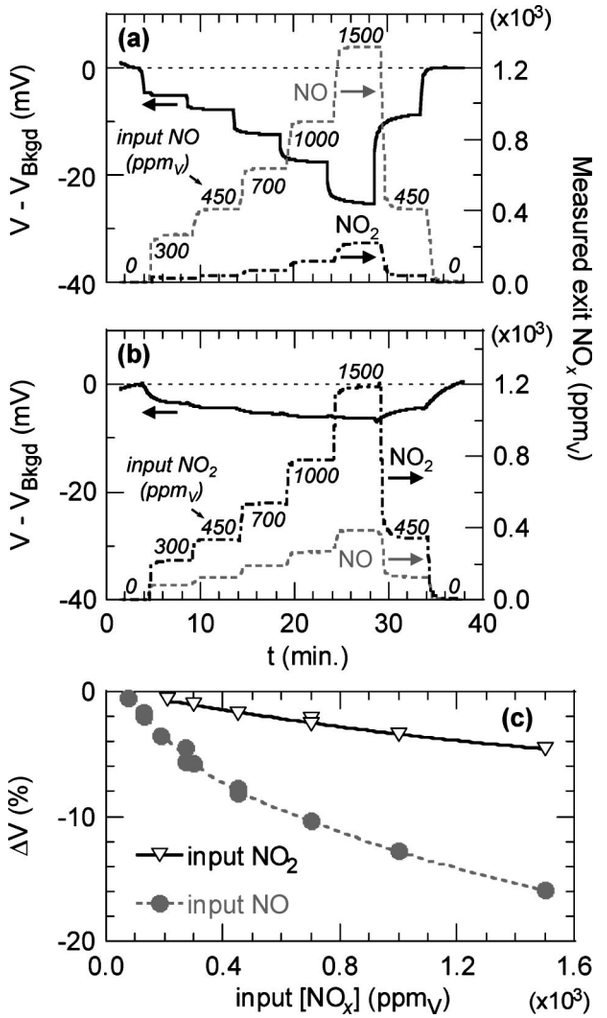

Figure 6. Comparison of NO and NO_2 responses at 600°C (7 vol % O_2) for current-biased sensing elements. (a and b) Show the response traces with input (a) NO and (b) NO_2 of a LCC sensing element biased with a dc current of +0.2 mA. The computed changes in voltage (ΔV, from V_{meas} with 0 ppmv NO_x) for a $CuWO_4$ sensing element with +0.18 mA bias are shown in (c). The data in (a) and (b) were background subtracted to eliminate drift between the [NO] and [NO_2] variations, and the lines drawn in (c) are polynomial fits.

then voltage biased with the approximate voltage measured at 7 vol % O_2 and 0 ppmv NO under current biasing (+0.19 V) and subjected to identical [NO] variations. The measured changes in V (current biasing) and I (voltage biasing) due to NO were then converted to changes in resistance using

$$\Delta R(I \text{ bias}) = (V' - V_0)/(V_0), \quad \Delta R(V \text{ bias}) = (I_0/I') - 1 \quad [6]$$

where V_0 and I_0 were the measured voltage and current at and 0 ppmv NO, and V' and I' were the measured voltage and current at any other [NO].

The computed changes in resistance using Eq. 6 are shown in Fig. 7. It can be seen there that current and voltage biasing yield similar results for the sensing response. Therefore, it would appear that biased sensing elements of the geometry shown in Fig. 1a are resistive elements, and perhaps it would be misleading to refer to them as potentiometric elements if current biased, or amperometric elements if voltage biased.

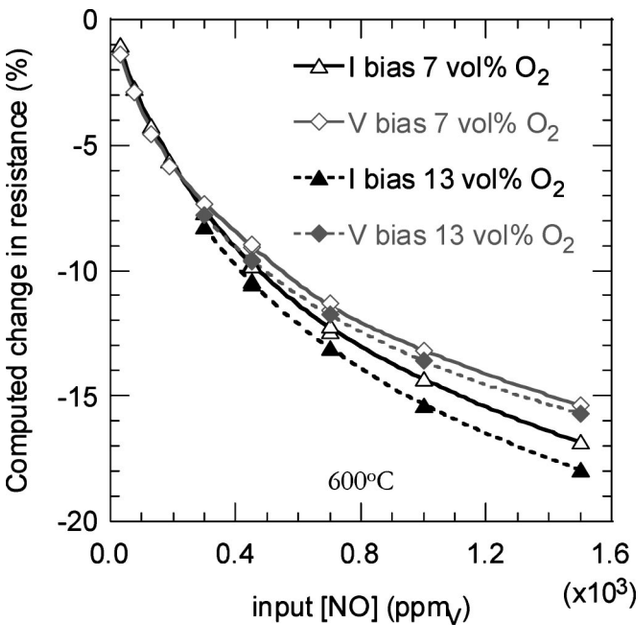

Figure 7. Measured changes in resistance as a function of [NO] for a $NiCr_2O_4$ sensing element with both voltage and current biasing. The lines drawn are polynomial fits.

Effect of varying [O_2].—The data in Fig. 7 suggest that [O_2] has little effect on the $NiCr_2O_4$ sensing element response over a wide NO concentration range. This is further borne out by the data in Fig. 8, which shows measured currents (with +0.2 V bias at 600°C) as a function of [O_2] (1-29 vol %) at fixed input [NO] levels of 0, 450, and 1500 ppmv. In general, varying [O_2] from 7 to 20 vol % had little effect on the measured current, irrespective of [NO], but decreasing [O_2] below 7% did decrease the measured currents with

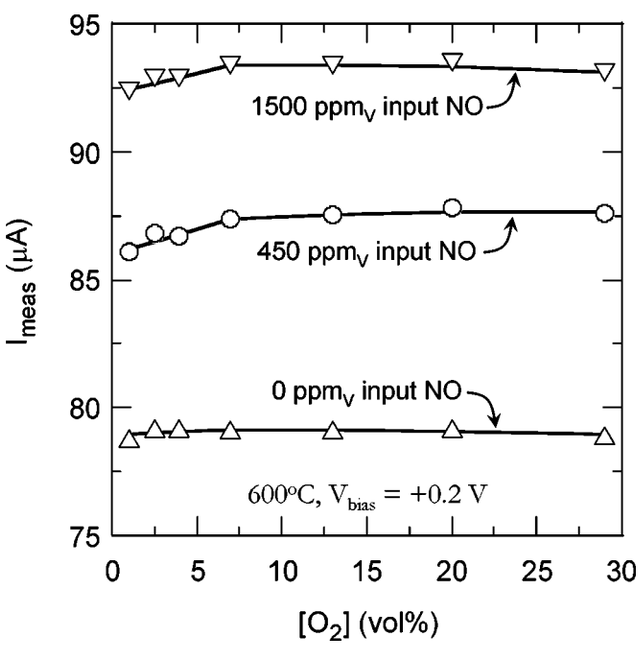

Figure 8. Measured currents with 0, 450, and 1500 ppmv input NO as a function of [O_2] for a voltage-biased (+0.2 V) $NiCr_2O_4$ sensing element operating at 600°C. Lines are drawn as an aid to the eye.

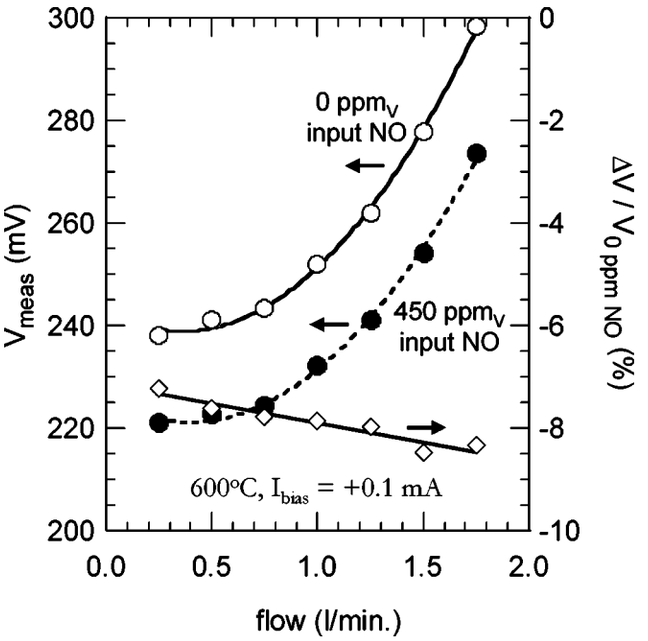

Figure 9. Measured voltages (V_{meas}) with both 0 and 450 ppm NO as a function of flow rate for a $NiCr_2O_4$ sensing element with +0.1 mA current bias. Also shown is the computed change in voltage ($\Delta V/V_{0\ ppm\ NO}$) due to the presence of 450 ppmv NO. The line fit to the percent change in voltage is a linear fit.

NO present. We should note that Miura *et al.*[11] and Ho *et al.*[12] observed little $[O_2]$ sensitivity for voltage-biased sensing elements operating at 500 and 400°C, respectively, when $[O_2]$ was varied between 5 and 40 vol %[11] or 5-20 vol %.[12]

The fact that with 0 ppmv NO the current is little affected by $[O_2]$ bolsters the assertion by Miura *et al.*[11] that the incorporation (or liberation) of oxygen (Eq. 3 and 5) into (from) the YSZ electrolyte is the rate-limiting step for current flow in these sensing elements. This would also be consistent with the presence of a relatively small amount of oxidizible (NO) or reducible (NO_2) species causing a large change in the dc electrical resistance of the sensing element.

Effect of flow rate on element response.—Figure 9 shows how the measured voltage (600°C, +0.1 mA bias, 7 vol % O_2, both 0 and 450 ppmv input NO) changed as a function of flow rate for a sensing element constructed with $NiCr_2O_4$ as the oxide. The measured voltages with both 0 and 450 ppmv input NO were strong functions of flow rate, but the change in voltage induced by NO ($\Delta V/V_{0\ ppm\ NO}$) was only weakly dependent on flow rate. It was also observed that the temperature recorded by the thermocouple in Fig. 1b varied by about 20°C as the flow was varied from 0.25 to 1.75 L/min, with the lower flow rate corresponding to the higher temperature. (At a fixed flow rate of 0.75 L/min, the thermocouple in Fig. 1b consistently indicated a temperature about 5°C lower than the set point of the furnace.)

In order to investigate further the furnace temperature was cooled from 630 to 570°C at 2°C/min with a constant +0.2 V bias, a flow rate of 0.75 L/min, and 7 vol % O_2, 0 ppmv NO_x in the test gas. Converting the measured currents during the cooling to resistances (R) and fitting against the inverse temperature recorded by the thermocouple (T_{sample}) in Fig. 1b yielded

$$R(\Omega) = (9.69 \times 10^{-4})\exp[(1.29 \times 10^{4})/T_{sample}] \qquad [7]$$

with T_{sample} in Kelvin. Figure 9 indicates that the resistance (with 0 ppmv NO) varied from about 3.0 kΩ at the highest flow rate employed (1.75 L/min) to about 2.4 kΩ at the lowest flow rate (0.25 L/min). Writing Eq. 7 with each of these resistance values and solving for the temperature difference (ΔT) indicates that these resistance changes correspond to a temperature change of *ca.* −13 K. Because this is close to the temperature difference that was recorded by the thermocouple in Fig. 1b, we attributed the changes in V_{meas} with flow rate observed in Fig. 9 to variations in element temperature. Temperature variations may also account for the slight increase in NO response with increasing flow rate seen in Fig. 9, because as noted earlier the NO response of these sensing elements was a decreasing function of temperature.

Conclusions

DC electrical biasing can greatly enhance the NO response of YSZ-based sensing elements with the geometry shown in Fig. 1a, and this has potential for applications in NO sensing of engine exhausts. Large responses (~10% changes in element response with 450 ppmv NO at 600°C) can be achieved using either voltage or current biasing, affording flexibility in sensor design. The element response is little affected by variations in $[O_2]$ between 7 and 20 vol %, which should be advantageous for applications in which the ambient $[O_2]$ is varying with time between these limits, as might be the case with diesel engine exhausts.

Acknowledgments

This project is funded by the U.S. Department of Energy Energy Efficiency and Renewable Energy's Office of Heavy Vehicle Technologies. The authors are grateful to C. A. Walls and B. L. Armstrong of Oak Ridge National Laboratory for fabricating the YSZ substrates and formulating inks for screen printing. The authors also acknowledge helpful discussions with D. Kubinski and R. Soltis of Ford Scientific Research Laboratories. Oak Ridge National Laboratory is operated by UT-Battelle, LLC for the U.S. Department of Energy under contract DE-AC05-00OR22725.

Oak Ridge National Laboratory assisted in meeting the publication costs of this article.

References

1. F. Menil, V. Coillard, and C. Lucat, *Sens. Actuators B*, **67**, 1 (2000).
2. N. Miura, M. Nakatou, and S. Zhuiykov, *Sens. Actuators B*, **93**, 221 (2003).
3. K. B. J. Schnelle and C. A. Brown, in *Air Pollution Control Technology Handbook*, p. 241, CRC Press, Boca Raton, FL (2001).
4. W. Gopel, R. Gotz, and M. Rosch, *Solid State Ionics*, **136-137**, 519 (2000).
5. N. Docquier and S. Candel, *Prog. Energy Combust. Sci.*, **28**, 107 (2002).
6. N. Kato, H. Kurachi, and Y. Hamada, *SAE Tech. Pap. Ser.*, 980170 (1998).
7. F. H. Garzon, R. Mukundan, and E. L. Brosha, *Solid State Ionics*, **136-7**, 633 (2000).
8. N. Miura, G. Lu, and N. Yamazoe, *Solid State Ionics*, **136-7**, 533 (2000).
9. A. Kunimoto, M. Hasei, Y. Yan, Y. Gao, T. Ono, and Y. Nakanouchi, *SAE Tech. Pap. Ser.*, 1999-01-1280 (1999).
10. G. Lu, N. Miura, and N. Yamazoe, *Sens. Actuators B*, **65**, 125 (2000).
11. N. Miura, G. Lu, M. Ono, and N. Yamazoe, *Solid State Ionics*, **117**, 283 (1999).
12. K.-Y. Ho, M. Miyayama, and H. Yanagida, *J. Ceram. Soc. Jpn.*, **104**, 995 (1996).
13. M. L. Grilli, E. Di Bartolomeo, and E. Traversa, *J. Electrochem. Soc.*, **148**, H98 (2001).
14. V. Coillard, H. Debeda, C. Lucat, and F. Menil, *Sens. Actuators B*, **78**, 113 (2001).
15. J. Kaspar, P. Fornasiero, and N. Hickey, *Catal. Today*, **77**, 419 (2003).
16. M. Zheng, G. T. Reader, and J. G. Hawley, *Energy Convers. Manage.*, **45**, 883 (2004).
17. K. C. Patil, S. T. Aruna, and S. Ekambaram, *Curr. Opin. Solid State Mater. Sci.*, **2**, 158 (1997).